Efficient Braking Model for Off-road Mobile Robots

Mihail Pivtoraiko, Alonzo Kelly, Peter Rander, John Bares

Robotics Institute Carnegie Mellon University Pittsburgh, PA 15213-3890

email: alonzo@ri.cmu.edu, url: http://www.frc.ri.cmu.edu/~alonzo

Abstract

In the near future, off-road mobile robots will feature high levels of autonomy which will render them useful for a variety of tasks on Earth and other planets. Many terrestrial applications have a special demand for robots to possess similar qualities to man-driven machines: high speed and maneuverability. Meeting these requirements in the design of autonomous robots is a very hard problem, partially due to the difficulty of characterizing the natural terrain that the vehicle will encounter and estimating the effect of these interactions on the vehicle. Here we present a dynamic traction model that describes vehicle braking on a variety of terrestrial soil types and in a wide range of natural landscapes and vehicle velocities. This model was developed empirically, it is simple yet accurate and can be readily used to improve model-predictive planning and control. The model encapsulates the specifics of wheel-terrain interaction, offers a good compromise between accuracy and real-time computational efficiency, and allows straight-forward consideration of vehicle dynamics.

1 Introduction

As developing autonomous off-road vehicle technology allows robots to travel at higher speed and negotiate rugged terrain, vehicle modeling becomes increasingly relevant for motion planning and control. An efficient braking traction model can greatly enhance vehicle autonomy by addressing two key problems: it can determine whether the path ahead, given its slope and ground characteristics, presents risks such as tip-over, and provide a precise estimate of the stopping distance. Precision of the model is very important, but it should also be very efficient computationally because it has to be continually evaluated if it is used for control or tightly coupled with the path planning algorithm. Certainly, a gross over-estimation for the problems above will likely keep the vehicle safe, however in cluttered natural terrain such approach will either result in slow, inefficient traversal, or may cause a failure of the path planner to generate an admissible path.

1.1 Prior Work

A great deal of research has been done in interaction of pneumatic tires with the ground. Good tire models have been developed for the automotive industry ([10], [21], [22]) and work quite well for applications on paved sur-



Figure 1: The PerceptOR off-road mobile robot. The experiments were performed with vehicles similar to the one pictured here.

faces. Off-road conditions certainly make things more difficult; [1] and [4] offer great overviews of automobile off-road mobility and probabilistic approaches to soil modeling. Whereas these approaches may be quite general by virtue of including fairly complex wheel-terrain equations of many parameters that depend on various classes of soil, they may not necessarily be the best for model-based motion planning. Typically in model-predictive planning, many candidate robot trajectories are considered and an optimal trajectory in some sense is chosen. In this regard, an accurate but complicated model will cause this evaluation process to be much too slow for applications in real mobile robots. Moreover, it is often not possible to determine all the many necessary model parameters ahead of time.

Quite a few fairly detailed models of the wheel-soil interaction were proposed specifically for motion planning applications. For example, [5], [6], [7] and [19] present approaches that model the soil as a mass-spring system, where the soil granules are considered as point-masses, and interaction between them is modeled by spring force. These models provide fairly good results in describing compression, shear and plastic deformations in soils. They also help estimate many useful properties of loose soils and explain traction of peristaltic motion [2]. However, these approaches are yet to be thoroughly verified experimentally. Moreover, the reported run-times of these modeling methods do not appear to be fast enough to render them feasible in real-time robot control scenarios.

The approaches that were shown to be suited for controlling mobile robots tend to circumvent the issue of computational efficiency by further simplification. Usually the Coulomb principle of friction, or its derivative is used to estimate the amount of rolling friction that the vehicle experiences. [12] assumes that tread on the wheels is large and the vehicle moves fairly slowly so that there is always very good contact with loose soil. Several parameters of the terrain are used in [15] to estimate normal and lateral tangential forces at the wheel contact patch. A similar approach to traction modeling that can also be adapted online was presented in [14], and similar issues are treated in [26]. This work is focused on planetary applications with accompanying quasi-static assumptions. Also, it is assumed that metal wheels are used and that terrain is smooth, so that it is possible to consider the wheel to be rigid. Pneumatic tires used for terrestrial applications, however, are elastic. Morever, in off-road applications the inflation pressure is typically quite low in order to avoid rigid-mode operation that may cause excessive compaction of soil [4]. To our knowledge there is no published work in fast systematic approaches to estimating wheel-terrain friction with respect to braking deceleration that was also validated on robots in a variety of natural terrestrial environments.

1.2 A New Approach

We conducted a significant field experimentation effort with autonomous off-road robots, and this prompted an empirical approach to capturing the complexities of wheel-terrain dynamics in natural environments. An initial observation was that it was generally not possible to consider the overall braking force of the vehicle (with gravity effects removed) to be some constant value. In fact, in some cases on soft soil the net braking force (no gravity effects) on a slope was off by as much as 50% from its value on level ground. Depending on vehicle dynamics, this can result in a miscalculation of the stopping distance by several meters, which may be a serious error when operating in cluttered natural terrain.

We propose an approach that provides accurate estimates of tractive braking force and involves a simple and efficient model of several parameters. The values of the parameters are determined experimentally by measuring the deceleration during vehicle braking and combining these measurements with vehicle state information. This "training" procedure can be easily done in the field, and even autonomously by the robot. For example, every time the robot has to stop, it can verify its braking model. In this manner, the model can be refined on-line and adapted as the robot moves into different type of terrain. This formulation of the model was shown to work well on off-road robots operating on a wide variety terrain types, such as clay, soil with sod cover, gravel, coarse sands, and packed snow, as well as at various speeds and on natural slopes (typical to mid-West region, the plains and the desert).

This model can be used in model-predictive control to estimate the *stopping path* ([16], [17]), the guaranteed stopping distance that is necessary for vehicle safety, which is mainly a function of a complex relationship between vehicle speed, tire-ground interface, and terrain slope. The model can also be utilized by the path planning algorithm to generate plans that respect this stopping path ([5], [6]). Since the present model also estimates major forces acting on the vehicle during braking maneuvers, it can also be used in kinodynamic motion planning approaches [8]. Moreover, if an estimate of tire sliding friction coefficient

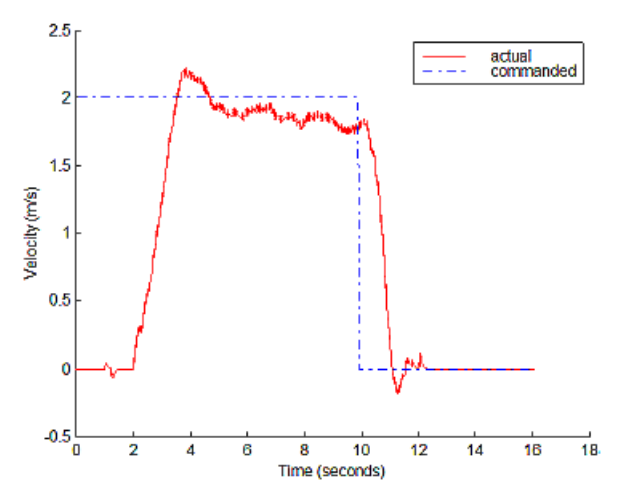


Figure 2: Deceleration measurement experiment. Blue dotted line shows commanded velocity of 0 (at t=10), and red line shows system response.

is available, then this model can predict whether robot's wheels are going to lock up (which generally must be avoided [25]).

2 Experimental Procedure

In this section we give the details of experiments that prompted us to formulate this model of braking. In our experiments, a terrain patch that is a good representative of the overall terrain is chosen (often natural environments have fairly uniform type of ground over large areas: meadows, field, desert, etc.). The vehicle accelerates to a certain value of velocity, v_t , and then applies the brakes with some known force (either maximum application for vehicles that have no braking force feedback, or a certain known value for those that do). Most vehicle control systems with closed-loop velocity control estimate velocity more frequently than it can significantly change, so it is possible to achieve the temporal resolution sufficient to obtain the velocity profile of vehicle stopping. The velocity data can be plotted against time as in Figure 2. Note that actual velocity in the plot goes slightly negative after reaching zero. This is due to expansion of suspension springs that were compressed during braking.

The time when braking was initiated (when desired velocity is set to zero) is recorded, along with the time when velocity reached zero, t_f . The average value of deceleration in the particular experiment is estimated as shown in (1).

$$\bar{a} = \frac{v_i}{t_f - t_i} \tag{1}$$

The value \bar{a} is the slope of the velocity drop in the figure. In this calculation, it is important to note that, as can be seen in Fig. 6, there is a certain delay after the system commands a zero velocity to when the velocity actually begins to drop. This delay of propagation of the command, t_{delay} , depends solely on hardware. It was on average 0.3 sec. on our robots. For braking at higher speeds, it is much less than overall Δt , yet needs to be taken into account. Therefore, we take t_i as time of zero-velocity command plus t_{delay} , and sample v_i specifically at that value of t_i to obtain an accurate estimate of the slope.

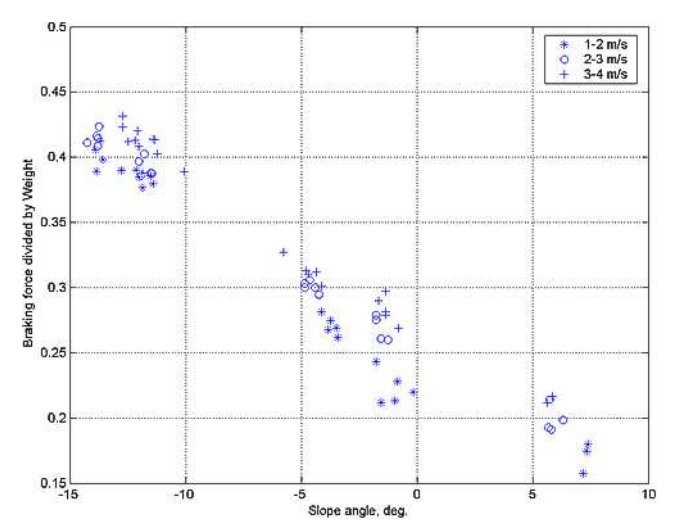


Figure 3: Normalized braking force, ${\it F_b/W}$, versus ground slope and vehicle velocity.

Throughout our experiments we made sure that the degree of brake engagement was constant. In particular, we were interested in maximum braking, i.e. in engaging the brakes completely.

The same experiment was then repeated with various vehicle velocities and on the ground of various slopes and terrain types. We fitted the above data gathering procedure in the robots' controller code, so that we could obtain a data point at any time when the robot made a stop. In this manner we obtained the data over several months as the robots were used for a variety of navigation and perception experiments on the PerceptOR program. Thus we obtained thousands of data points that were then analysed.

If we plot the measurements of decelerations versus slope for a choice of terrain and subtract the effects of gravity, we see that the resulting net braking force slightly increases with the increase of slope angle, as we expected in our analysis above. An example plot is presented in Figure 3, which shows the normalized braking force, a ratio of breaking force to vehicle weight F_b/W , as a function of slope and velocity. The dependence of deceleration on initial velocity is also noticeable, albeit not as pronounced. Interestingly, these data points exhibit proportional dependence of normalized braking force to slope angle. Hence, a single linear model should be able to predict the braking force for both downhill and uphill braking maneuvers.

Note, however, that our observations have been made in tests on slopes well within limits of vehicle traversability, which was about 20 degree slopes for our hardware. It is natural to expect that beyond this range of slope values the dependence is no longer linear.

Also, on some vehicles it may occur that the coefficient of proportionality of braking force to slope angle is different for braking downhill and uphill. We believe that creating a separate model for either case will be quite doable since it is a simple matter to find the coefficients of the linear dependence as described above.

3 Discussion of Results

In this section we develop the necessary concepts to under-

stand the factors influencing traction during vehicle braking. We then use the developed concepts in an effort to explain our experimental observations and suggest a model based on this analysis.

3.1 Vehicle Force Balance

As a starting point, we develop simple force analysis of the vehicle during braking. Among the important notions that we define here are normal forces on tires, pressure of the tire contact patch, and the dynamic load transfer.

During braking, the major forces acting on the vehicle are related through:

$$F_b = W \frac{a_x}{g} - W \sin \theta \tag{2}$$

where F_b is the net braking force, g is acceleration due to gravity, a_x is braking deceleration, $W = m_{veh}g$ is vehicle weight, and θ is the terrain slope angle (here we consider downhill slopes as negative, and uphill as positive). The first term on the right side of (2) is the d'Alembert force [11] (see Fig. 4).

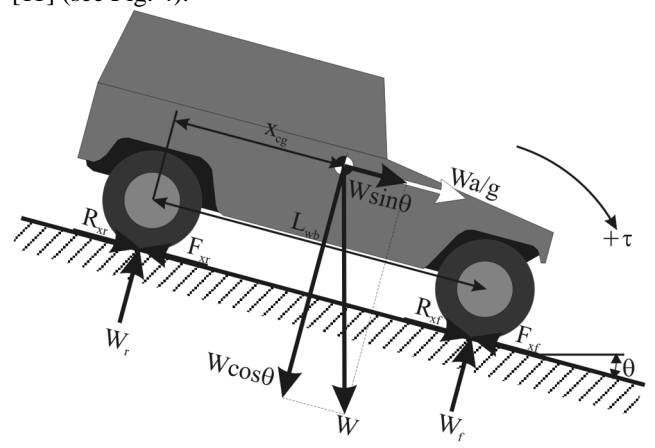


Figure 4: Free body diagram of a vehicle braking on a slope. Positive torque is assumed clockwise.

Given that the vehicle center of gravity, (x_{cg}, y_{cg}, z_{cg}) , is known, we can express the sum of torques around the contact point of front wheels (for downhill slopes, assuming positive torque is clockwise):

$$-(L_{wb} - x_{cg})W\cos\theta + W_r L_{wb} + z_{cg}W_{g}^{a} + z_{cg}W\sin\theta = 0$$
 (3)

Here L_{wb} is wheel base, and w_r is weight on the rear axle. When the vehicle is stationary on level ground, the loads on front axle, w_{fs} , and rear axle, w_{rs} , are determined by:

front axle,
$$w_{fs}$$
, and rear axle, w_{rs} , are determined by:
$$W_{fs} = W \frac{L_{wb} - x_{cg}}{L_{wb}} \qquad W_{rs} = W \frac{x_{cg}}{L_{wb}} \tag{4}$$

In case of a vehicle decelerating on a slope, we obtain the normal forces on rear and front wheels by summing the torques around front and rear wheel contact points, respectively:

$$W_f = \frac{W}{L_{wb}} \left(x_{cg} \cos \theta + x_{cg} \sin \theta + z_{cg} \frac{a_x}{g} \right)$$
 (5)

$$W_r = \frac{W}{L_{wb}} \left((L_{wb} - x_{cg}) \cos \theta - z_{cg} \sin(-\theta) - z_{cg} \frac{a_x}{g} \right)$$

We observe from (5) that during braking downhill, there is a significant dynamic load shift from rear to front axles. Note that w_r was written with the $z_{cg}\sin(-\theta)$ term to underscore the fact that for downhill slopes $\theta < 0$.

We consider pressure on the tire contact patch for front and rear wheels as the ratio of axle load to contact area. The vehicles we had available for experiments in this study had dual rear tires, so we estimate that the pressure of front tires' ground contact was twice that of rear tires.

3.2 Braking Force

Typically the work required to slow down a vehicle is done by the friction force inside the braking mechanism. Suppose that the braking torque results in a longitudinal force F_h at the wheel-terrain interface. Since the goal of this work was to understand the effects of maximum braking that determines minimum allowable stopping distance and outlines the upper bound on dynamics effects due to braking, we understand that F_h represents full engagement of the brakes and depends solely on braking *hardware*, hence always constant. Here we also assume that braking happens on a straight path. We visualize the effect of this force in the detail of interaction of an off-road tire with terrain in Figure 5.

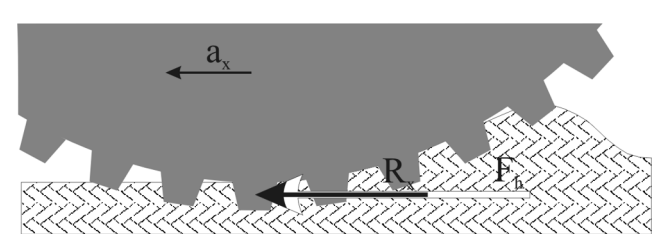


Figure 5: Detail of wheel-terrain interface. We focus on two dominating forces: braking traction force F_h and rolling resistance $R_{\rm r}$.

The hardware braking force F_h is counter-acted by the terrain acting on tire tread. If the magnitude of this force exceeds the shear strength of the terrain, it will no longer be able to resist this shear force, and the wheel will skid.

The other force in the tire-ground interface that was found to have significant effect on braking is rolling resistance R_x . This resistance is always present, and in the case of pneumatic tires its value is determined by many factors, such as tire material and design, temperature, vibration, pressure of the ground contact patch (normal force on the tire). Terrain compaction (related to pressure of the patch) and bulldozing effects in soft soil are also major contributing factors to this resistance [4]. While F_h can be considered constant for a given vehicle, estimating R_x is complicated due to the variety of factors influencing it.

Through experimentation we found that we can approximate all longitudinal forces acting on the vehicle during braking by lumping them into the sum of the force due to the torque supplied by the braking hardware, and the rolling resistance. Then, the overall braking force is considered to be:

$$F_b = F_h + R_x \tag{6}$$

The key to accurately predicting the braking force is estimating rolling resistance $R_{\rm r}$.

In our experiments it was also determined that out of all factors influencing rolling resistance, the most significant one is the pressure at ground contact. A lesser, but noticeable, effect has vehicle speed. In the following two sections we explain these two factors.

3.3 Effect of Terrain Slope

It is important to consider contact pressure here because in general rolling resistance is roughly proportional to this pressure (although this relationship is complex and highly non-linear) [1], [4].

For the case of level ground we can decompose (6) into the contributions of front and rear wheels:

$$F_b = 2F_h + R_{xr} + R_{xf}$$

Here F_h is the same for front and rear wheels since our vehicles had the interlocked differential. Also our robots had dual rear tires, which resulted in twice the contact area and half the ground contact pressure for rear tires than for the front tires. Hence, let us suppose (only for clarification purposes in this section) that due to the difference in contact pressures, the rolling resistance values can be related through $R_{xf} = 2R_{xr}$.

As was shown earlier, during downhill braking there is a significant dynamic load shift to front wheels, $w_r < w_f$. Because of this the pressure developed at front wheel contact point greatly exceeds that at rear wheel contact, and even more so in the case of rear dual tires. R_{xf} increases dramatically, more than R_{xr} decreases (in part due to half the contact pressure). The overall value of F_b becomes greater than on level ground.

During braking uphill, similar issues come into play. However, in this case the load shift to front axle is less significant (see (5)), in fact even less than on level ground due to $x_{cg} \sin \theta$ term and because braking deceleration in these vehicles was not very high. In this case $w_r > w_f$, whereas for level ground we had $w_r = w_f$. However, since rear tires have "half the effect" on rolling resistance than the front tires, the overall braking force is less than on level ground.

3.4 Effect of Velocity

Among the factors influencing rolling resistance is vehicle velocity [11]. The rolling resistance is directly proportional to velocity because of increased tire deformation work and vibration in the tire. The influence of velocity becomes more significant when tires with lower inflation pressures are used, as is often the case for off-road vehicles. Lower tire pressure is used to allow tires to be more elastic, since the work required for flexing the tire is much less than the work of compacting and bulldozing soft soil. Greater elasticity, however, causes greater hysteresis losses with increasing vehicle velocity. The effect of velocity on rolling resistance was found to be less significant, but still noticeable.

4 Deriving the Model

In this section we combine our experimental observations with the insights developed above to formulate our model of braking force. We describe how this model could be easily adapted online and discuss the results of validating the

model through experiments with robots.

4.1 Formulating the Model

As we discussed, the results of our experiments prompted us to make a simplifying assumption that within the range of slope values that the vehicle can safely handle, the braking force is proportional to the slope.

The essence of our model is stated as:

 The braking force (without gravity effects) can be approximated well by a linear model:

$$\frac{\partial F_b}{\partial \theta} = m$$

where θ is ground slope angle and m is a coefficient. We can fit a line $F_b = m\theta + b$ to the test data in the least-squares manner and use it to obtain future estimates of F_b based on slope.

• The coefficients *m* and *b* above also exhibits linear dependence on initial velocity of the vehicle (right before braking is initiated):

$$\frac{\partial m}{\partial v_i} = m_m \qquad \frac{\partial b}{\partial v_i} = m_b$$

Thus, the overal model contains only four parameters: m_m , m_b , b_m , and b_b :

$$m(v_i) = m_m v_i + b_m$$

$$b(v_i) = m_b v_i + b_b$$
(7)

So that

$$F_b = m(v_i)\theta + b(v_i) \tag{8}$$

We again underscore that the development of the model was based on experimental data, which was available for a range of terrain slope roughly from -15° to 15°. While this model cannot be extrapolated outside the experimental range in which it was defined, we can reason about the character of F_h outside of this range. In particular, based on previous discussion, we estimate that for greater uphill slopes, the effect of rolling resistance will diminish due to decreasing normal force, i.e. contact pressure, and F_b will approach F_h (omitting gravity effects, as usual). At a certain point the slope becomes unsafe, when the shear capacity of the wheel-terrain interface becomes equal to F_h . For steeper downhill slopes similar arguments apply: rolling resistance will become less dominant with decreasing soil contact pressure, and at some point the shear capability may no longer support the vehicle.

In the experiments that lead to formulation of this model, we have assumed that the degree of application of the brakes was constant throughout the experiments (e.g. for emergency braking, which often determines the look-ahead distance for a path planner, maximum actuator power is used). For other actuator modes this model is also applicable, but additional coefficients may be necessary to allow for other than maximum braking (e.g. slight, half way, etc.). On the other hand, the benefits of this expression of the model are that it is very simple and intuitive, quite easy to adjust, yet powerful enough to account for peculiarities of braking hardware and ground types, while requiring very low online computational overhead.

4.2 Adaptive Calibration of the Model

In order to enable the robot to adapt its braking traction model to the terrain that may be changing, we measure average deceleration during each time the brakes are engaged. This measurement, along with estimates of current pitch angle and velocity (available from robot's state estimator) are used as ground-truth to verify and update the model. A sizeable collection of these data-points is gathered during vehicle operation. There are several popular methods and learning techniques to solve this problem quite well. We have implemented a simple least-squares estimator that uses this collection of data points to refine the estimates of the four parameters of our model.

First we use the measured average deceleration \bar{a} and slope angle θ to estimate ground-truth values of slope-dependent parameters m and b.

We let the vector $\mathbf{a} = [\overline{a_1}, \overline{a_2}, ..., \overline{a_n}]^T$ contain n measurements of deceleration, and $\Theta = [\Theta_1, \Theta_2, ..., \Theta_n]^T$, where $\Theta_i = \begin{bmatrix} \theta & 1 \end{bmatrix}$. Then we estimate the parameters as

$$\begin{bmatrix} m_i \\ b_i \end{bmatrix} = (\boldsymbol{\Theta}^T \boldsymbol{\Theta})^{-1} \boldsymbol{\Theta}^T \boldsymbol{a} \tag{9}$$

Once we have these parameters, we proceed similarly to estimate velocity-dependent parameters:

$$M = \begin{bmatrix} m_1 & m_2 & \dots & m_n \end{bmatrix}^T$$

$$V = \begin{bmatrix} V_1 & V_2 & \dots & V_n \end{bmatrix}^T \qquad V_i = \begin{bmatrix} v_i & 1 \end{bmatrix} \qquad (10)$$

$$\begin{bmatrix} m_m \\ b_m \end{bmatrix} = (V^T V)^{-1} V^T M$$

We do exactly the same to obtain the coefficients m_b and b_b .

Depending on the mission, the robot may do quite a few stops and assemble a fairly large collection of data points. To make certain that memory data buffer does not overflow, it may be beneficial to use a FIFO data buffer of certain length.

4.3 Experimental Results

This model was verified on available data and through a series of new experiments: braking on level ground, downhill and uphill, at velocities in the range (1, 4) m/s, and with 10 repetitions of each test to ensure correlation (with this approach it was confirmed that results from repetitions had very little variability). Afterwards, the model was tested on the same terrain through long autonomous runs where the system issued a total of about 200 complete stop commands. The results are presented in Fig. 6 (the horizontal axis represents stop number).

Note that the predicted value of stopping distance is always above the actual, which is always necessary to keep the vehicle safe. The overestimation is on average about 50cm and can be controlled through the s_{offset} parameter (see (12)). The first 45 stops in the plot have quite a bit higher stopping distances as they were done at higher velocities (in excess of 3m/s) and on downhill slopes. The rest of the data is from the usual operation of these particular vehicles: about 2 m/s velocity and on slopes in the range (-15°, 15°). Thus, while the model is quite easy to tune and calculate in real time, it provides a fairly accurate prediction of vehi-

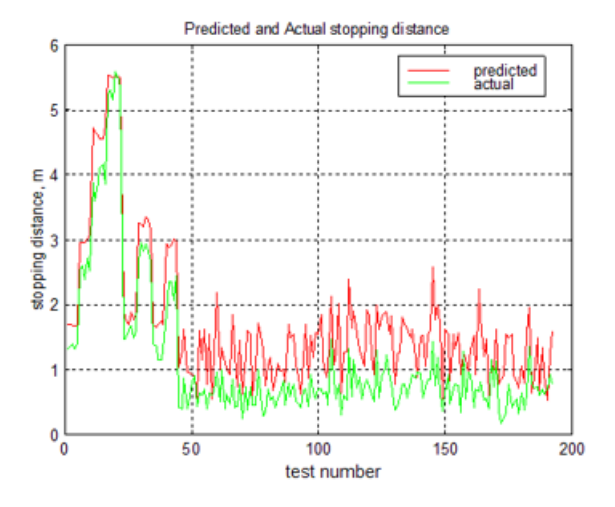


Figure 6: Comparison of predicted and actual stopping distance. cle's deceleration given its state and the predominant type of soil.

5 Applications of the Model

The main motivation for estimating a braking model was the determination of the stopping distance. Here we give formulas for computing both stopping time and distance. Another important application of the model is estimation of vehicle dynamics during braking. Once the balance of forces is known, it becomes possible to answer questions about whether a particular slope is viable for the vehicle (e.g. in terms of tip-over hazard).

5.1 Estimating Stopping Distance and Time

Average braking deceleration a_x can be obtained from (2) once we have an estimate for braking force F_b .

Since deceleration is negative change of velocity over time, we estimate the stopping time, t_c , given deceleration, a, as

$$t_s = \frac{v}{a} + t_{delay} + t_{offset} \tag{11}$$

where t_{offset} is an offset to ensure that the result is always somewhat overestimated in order to keep the vehicle safe.

Similarly, stopping distance, s_s is calculated based on the fact that deceleration is the second time derivative of distance:

$$s = \frac{1}{2}at_s^2 + t_{delay}v + s_{offset} \tag{12}$$

where s_{offset} is a similar distance offset.

5.2 Predicting Vehicle Tipover Condition

Calculating tip-over condition involves finding the sum of torques around the point of contact of front wheels of the vehicle (refer to (3) and Fig. 4). To find the threshold where the vehicle will start to tip over, we need to find when the weight acting on the rear axle, w_r , becomes zero. However, practically the vehicle will be in danger even before this condition occurs. When the normal force w_r , becomes low enough so that the sliding friction force caused by it

becomes equal to the braking force, rear wheels will start sliding and a loss of directional stability will occur [25]. When this happens, the capability of the rear tires to resist lateral force is reduced to zero, and a yawing moment due to a slight centrifugal force or other effects will develop the inertia force about the yaw center of the front axle. Therefore, to find a more suitable estimate of maximum allowable slope angle, we have to solve the equation (3) for θ so that $|W_r|$ is equal to a relatively small value greater than 0. This will require us to solve an equation of the form $A\cos\theta + B\sin\theta = C$ for θ . However, depending on required accuracy it is possible to simplify the equation significantly using small angle approximations.

The resulting θ is the maximum allowable pitch angle of the vehicle to prevent tip-over, given the longitudinal location of its center of gravity and other parameters. Since most of the components of equation (3) can be precomputed in advance, the estimation presents low computational overhead.

6 Conclusion and Future Work

We presented an empirical braking model that is very simple to estimate, yet produces quite accurate results that exhibit appreciably small errors in a very wide variety of off-road operation: high and low speeds, level ground and steep slopes that high-traction vehicles can negotiate. The model can also be extended with more analytical approaches that utilize estimation of soil sinkage and other peculiarities of navigating over soft, soils and sands. Also, popular tire models can be utilized for operations on hard surfaces. Our future work will involve testing the model on vehicles that can operate at much higher speeds and steeper slopes. We would also like to extend this study to maneuvers including steering while braking and acceleration (speeding up as well as slowing down). We hope to look into the application of more powerful learning techniques to adapting the model to the variety of natural terrain. Although the specifics can vary and further build on the simple empirical model, the spirit remains the same: a runtime characterization of vehicle dynamics that can support many intelligent decisions on the part of a vehicle path planning system operating in unpredictable off-road environments.

7 References

- [1] Ia.S. Ageikin, Off-the-road Mobility of Automobiles, A.A.Balkema, Rotterdam: 1987.
- [2] G. Andrade et al. "Modeling Robot-Soil Interaction for Planetary Rover Motion Control". In Proc. of the Int. Conf. on Intel. Robots and Systems, Victoria, B.C., Canada, October 1998.
- [3] B. d'Andrea-Novel, M. Ellouze. "Tracking with Stability for a Vehicle Braking in a Corner". Proceedings of the 40th IEEE Conference on Decision and Control, Orlando, Florida USA, December 2001.
- [4] M. Bekker. *Introduction to Terrain-Vehicle Systems*. University of Michigan Press, 1969.
- [5] B. Chanclou, A. Luciani, A. Habibi. "Physical Models of Loose Soils Dynamically Marked by a Moving Object". In Proc. of the Int. Conf. on Robotics and Automation, 1996.

- [6] B. Chanclou, A. Luciani. "Global and Local Path Planning in Natural Environment by Physical Modeling". In Proc. of the Int. Conf. on Intel. Robots and Systems, 1996
- [7] B. Chanclou, A. Luciani. "Physical Modeling and Dynamic Simulation of Off-Road Vehicles and Natural Environments". In Proc. of the Int. Conf. on Intel. Robots and Systems, 1996.
- [8] B.R. Donald, P.G. Xavier, J. Canny, J. Reif, "Kinodynamic planning," Journal of the ACM, v.40, pp. 1048-1066, Nov. 1993.
- [9] S. Farritor, H. Hacot, S. Dubowsky. "Physics-Based Planning for Planetary Exploration". In Proc. of the Int. Conf. on Robotics and Automation, Leuven, Belgium, May 1998.
- [10] M. Gafvert, J. Svendenius. "Construction of Novel Semi-Empirical Tire Mobels for Combined Braking and Cornering". ISRN LUTFD2/TFRT7606SE.
- [11] T.D. Gillespie, Fundamentals of Vehicle Dynamics, SAE: 1992.
- [12] K. Iagnemma et al. "Experimental Validation of Physics-Based Planning and Control Algorithms for Planetary Robotic Rovers". In Proc. of the Int. Symposium on Experimental Robotics, 1999.
- [13] K. Iagnemma, F. Genot, S. Dubowsky. "Rapid Physics-Based Rough-Terrain Rover Planning with Sensor and Control Uncertainty", In Proc. of the Int. Conf. on Robotics and Automation, 1999.
- [14] K. Iagnemma, H. Shibly, S. Dubowsky. "On-Line Terrain Parameter Estimation for Planetary Rovers". In Proc. of the Int. Conf. on Robotics and Automation, May, 2002.
- [15] A. Jain et al. "Recent Developments in the ROAMS Planetary Rover Simulation Environment". IEEE Aerospace Conf., Big Sky, Montana, March 6-13, 2004.
- [16] A. Kelly, A. Stentz. "Rough Terrain Autonomous Mobility - Part 1: A Theoretical Analysis of Requirements", Autonomous Robots, v.5, pp.129-161, 1998.
- [17] A. Kelly, A. Stentz. "Rough Terrain Autonomous Mobility - Part 2: An Active Vision, Predictive Control Approach", Autonomous Robots, v.5, pp.163-198, 1998.
- [18] U. Lages. "Collision Avoidance System for fixed Obstacles", IEEE Intelligent Transportation Systems Conference Proceedings, Oakland, Augusts 2001.
- [19] A. Luciani, B. Chanclou. "Physical Models of Off-Road Vehicles Moving on Loose Soils". In Proc. of the Int. Conf. on Intelligent Robots and Systems, 1997.
- [20] T. Muro, T. Shigematsu, "Automation and optimal design method of a wheeled vehicle operating over sloped weak sandy terrain," Automation in Construction, 2000.
- [21] B.J. Olson, S.W. Shaw, G. Stepan, "A Nonlinear Model for Vehicle Braking," in Proc. of 8-th Conference on Nonlinear Vibrations, Stability, and Dynamics of Structures (Blacksburg, VA), 2000.
- [22] H.B.Pacejka, ed. *Tyre Models for Vehicle Dynamics Analysis*, Swets&Zeitlinger B.V., Amsterdam/Lisse: 1993
- [23] A.S. Shkel, V.J. Lumelsky, "Incorporating Body Dynamics Into Sensor-Based Motion Planning: The Maximum Turn Strategy," IEEE Transactions on Robotics and Automation, vol. 13, No. 6, Dec. 1997.

- [24] K. Terzaghi, Theoretical Soil Mechanics, Wiley, New York, 1943.
- [25] J.Y. Wong, *Theory of Ground Vehicles*, 2nd ed., Wiley, 1993
- [26] K. Yoshida, G. Ishigami, "Steering Characteristics of a Rigid Wheel for Exploration on Loose Soil," in Proc. of the Int. Conf. on Intelligent Robots and Systems, 2004